Modelling Extreme Concentrations from a Source in a Turbulent Flow over a Rough Wall

Zhengtong Xie [a][1]   Paul Hayden [b]
Alan G. Robins [b]   Peter R. Voke [b]

[a]*School of Engineering Sciences, University of Southampton, SO17 1BJ, UK*

[b]*Fluids Research Centre, The University of Surrey, GU2 7QH, U.K.*

Abstract

The concentration fluctuations in passive plumes from an elevated and a ground-level source in a turbulent boundary layer over a rough wall were studied using large eddy simulation and wind tunnel experiment. The predictions of statistics up to second order moments were thereby validated. In addition, the trend of relative fluctuations far downstream for a ground level source was estimated using dimensional analysis. The techniques of extreme value theory were then applied to predict extreme concentrations by modelling the upper tail of the probability density function of the concentration time series by the Generalised Pareto Distribution. Data obtained from both the simulations and experiments were analysed in this manner. The predicted maximum concentration (Γ_0) normalized by the local mean concentration (C_m) or by the local r.m.s of concentration fluctuation (c_{rms}), was extensively investigated. Values for Γ_0/C_m and Γ_0/c_{rms} as large as 50 and 20 respectively were found for the elevated source and 10 and 15 respectively for the ground-level source.

Key words: large-eddy simulation, atmospheric dispersion, extreme value theory

1 Introduction

The significance of concentration fluctuations is recognized in principle but the incorporation of that understanding into predictive safety codes in a quantitative manner is by no means simple, owing to the turbulent nature of atmospheric flow and hence of the concentration distributions. Experimental

---

[1] Corresponding author. Email: z.xie@soton.ac.uk; tel: +44(0)23 8059 3334; fax: +44(0)23 8059 3058

evidence shows that the dose (the mean concentration integrated over the time of exposure) can give a substantial underestimate of the short-term effect of exposure to a toxic substance. A generalised dose, related to some higher power of concentration, is often more appropriate. Extreme concentration fluctuations then become critical in determining the generalised dose. Similarly, ignition of a flammable gas depends on the gas concentration falling within the flammable limits and the availability of sufficient ignition energy; the probability of ignition is therefore directly linked to the probability distribution of concentration.

Large eddy simulation (LES) is known as a most promising technical approach to simulate atmospheric flow and dispersion, because of the very large Reynolds number involved. However, we can normally only simulate atmospheric boundary layer (ABL) flows over a short duration (e.g. a couple of hours) by LES, owing to current computer capability and the resulting high expense of simulations. Lack of sufficient information of the upper tail of probability density distribution (PDF) can make the standard estimation of extreme events severely biased (Coles, 2001). Extreme value theory (EVT) is the branch of statistics concerned with modelling the tails of probability distributions and hence performing probability extrapolations. A typical application of the generalized extreme value distribution (GEV) is to fit the distribution to a series of maximum data (for instance, annual maximum rainfall). However, the technique of characterizing a GEV distribution just by using maximum data during some fixed period is obviously of low efficiency. Use of the Generalized Pareto Distribution (GPD) (Pickands, 1975) has been proposed to obtain higher data-use efficiency. EVT has been applied to the study of the maximum concentration in atmospheric dispersion with some success (Anderson et al., 1997; Mole et al., 1995; Munro et al., 2001; Smith, 1989). Even so, there are many open problems worthy of further study. In the current work, we applied LES and wind tunnel experiment to study the concentration field from elevated and ground-level sources over a rough wall. EVT, namely GPD was used to postprocess the data obtained from both the LES and experiments to predict extreme concentrations.

2   Governing equations of LES and discretizing scheme for dispersion

The method of generating turbulent flows over a rough wall was reported in our previous paper (Xie et al., 2004a). The filtered scalar equation is given as follows,

$$\frac{\partial c}{\partial t} + \frac{\partial u_j c}{\partial x_j} = \frac{\partial}{\partial x_j}\left[(K_s + K_m)\frac{\partial c}{\partial x_j}\right] \tag{1}$$

where K_s and K_m are the subgrid turbulent diffusivity and molecular diffusivity respectively. LES resolves the large scale eddies and models the small scale eddies, i.e. subgrid scale eddies. Ideally, the subgrid scale is chosen within the inertial subrange. Most previous LES studies of dispersion applied a subgrid eddy viscosity combined with a subgrid Schmidt number to calculate the subgrid turbulent diffusivity, e.g. Sykes and Henn (1992). Here, a constant subgrid Schmidt number is taken, $Sc_s = \nu_s/K_s$, where ν_s is the subgrid viscosity, which is modelled using a subgrid scale parameterization (Xie et al., 2004a). Sc_s is the subgrid Schmidt number. Numerical experiments have been performed to check the sensitivity to the subgrid Schmidt number, and we have found that values around 1.2 yielded very small variations in the results (of course, significant changes would be expected for large variations in Schmidt number). Equation1, including the subgrid parameterization, was discretized in time by using a second-order explicit scheme:

$$\frac{c^{n+1} - c^n}{\Delta t} = \frac{3}{2}H_T^n - \frac{1}{2}H_T^{n-1} \tag{2}$$

where $H_T = -\frac{\partial c u_j}{\partial x_j} + \frac{\partial}{\partial x_j}\left[(K_s + K_m)\frac{\partial c}{\partial x_j}\right]$. Note that n indicates the time steps and that this scheme is second-order in time at time step $n + 1/2$.

Equation 1 was discretized in space using a second-order finite-volume method. The diffusion part is solved by central differencing. Firstly, as the gradient of concentration may be very large within a plume, we must avoid numerical diffusion. Secondly, we must avoid generating negative concentration by the so-called overshoot from central differencing. Consequently, the SMART Bounded Quadratic Upwind Scheme (Waterson & Deconinck , 1995) was used to discretize the convection term in space.

3 Experimental and Numerical Settings

The experimental measurements of turbulent flow over a rough wall were obtained in the Fluids Research Centre 'A' tunnel at the University of Surrey (Xie et al., 2004a). We used ethane as passive scalar in the experiment. A source of diameter 4mm (outer) and 3.4mm (inner) was located at x=0, y=0. In the current paper, we refer to an elevated source (ES) and a ground-level source (GLS), located at z=177mm ($0.4439D$) and 2.25mm ($0.00698D$) respectively, where D is boundary layer depth. The concentration was measured mainly at five downstream positions $x = 230, 380, 630, 1080, 1500$ (mm), where vertical profiles and lateral profiles were obtained. A hydrocarbon measurement system, a Cambustion HFR400 Fast Flame Ionisation Detector, was used

to measure the concentration. The maximum sampling rate used for obtaining the concentration time series data and spectra was $1000Hz$.

The computational domain size used for LES was $4D \times 1.47D \times D$ with periodic boundary condition in the streamwise and lateral directions. We discretized the computational domain using a mesh $256 \times 128 \times 128$. As far as the passive scalar field was concerned, we considered that a $4D$ fetch for dispersion was not long enough, and therefore a technique was used to extend the scalar computational domain to $8D \times 1.47D \times D$, with a mesh $512 \times 128 \times 128$. We simply copied the instantaneous upwind half (from x=0 to 4D) of the turbulent flow field calculated using LES, to the downwind half (x=4D to 8D). Because a periodic boundary condition in the streamwise direction was imposed for the simulation of turbulent flow, this technique was easily implemented for the simulation of the scalar field. The technique reduced CPU time and computer memory requirements by about a factor of two. Note this mesh was much finer than that of Sykes and Henn (1992). The boundary conditions for the scalar were as follows: a Dirichlet boundary condition was applied at the inlet, a convective boundary condition at the outlet, zero flux condition at the other boundaries.

At the inlet of the LES domain, the scalar was prescribed in the form of a Gaussian function with standard deviation $7.8*10^{-4}D$. We chose a small value of standard deviation to make the source size equivalent to one grid-space in the vertical and lateral directions, which was comparable to the source size in the wind tunnel experiment. The elevated source (ES) was located at $z=0.4324D$, while the ground level source (GLS) at height $z=0.00784D$ was located at the second grid from the wall. Note that the very high resolution and the non-zero height of the ground-level source ensured that the plume was released into the region where most of the turbulence energy was resolved (Xie et al., 2004a).

4 Some results of dispersion

In the LES, once the turbulent flow field was well developed, the source was initiated to release the scalar. The sampling for statistical averaging started at a dimensionless time $1.4D/u_*$, where u_* is the friction velocity. The averaging time was $8.3D/u_*$ to obtain traditional statistical data.

Fig. 1 shows the relative concentration fluctuations for elevated and ground-level sources, where C_m is the maximum mean concentration and c_{rms} is the maximum r.m.s on the vertical central line ($y = 0$) at each x station. For the ES, both wind tunnel measurements and the LES model predicted larger relative intensities than Thomson's model (Thomson, 1990), which was pro-
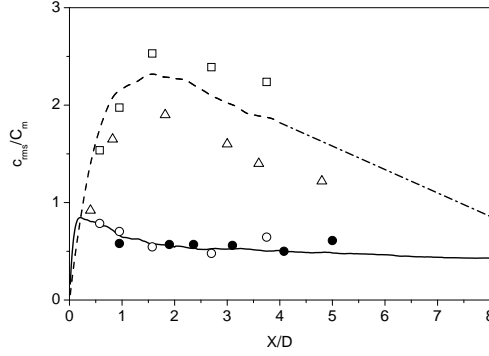
Fig. 1. Relative concentration fluctuations. □ measurements ES; △ Thomson's (1990) stochastic model ES; – – – LES ES; –·– extrapolated from LES ES; —— LES GLS; ○ measurements GLS; ● Fackrell and Robins (1982) GLS. C_m, c_{rms} maxima on vertical central line ($y = 0$) at each x station.

posed to suit the homogeneous turbulence. Brethouwer et al. (1999) predicted smaller relative intensities close to the source than Thomson's model and explained that the difference was the result of the low Reynolds number in their DNS as opposed to the infinite Reynolds number assumed in the model of Thomson.

The comparison between the LES and the experiment shows a discrepancy for both the ES and the GLS, which may be accounted for in several ways, such as the slight difference of resolution and source size. Some conditions of the Fackrell and Robins (1982) experiment were slightly different than those used in the LES, such as the Reynolds number and source size. Nevertheless, their measured relative fluctuations were comparable with the current LES and experimental data for the GLS. We noticed that the normalized velocity variances of Fackrell and Robins (1982) work were in agreement with the current experiment. Also note that the source size effect was not important for the GLS. These comments may explain the agreement in Fig. 1 for the GLS. We found that for the GLS there was a slight increase in the far field ($x/D > 3.5$) in the two experiments, which was due to the background signal noise that became important when the mean concentration decreased to a relatively low level.

Note in Fig. 1, the far downstream trend for ES is quite different from that for GLS. Sykes and Henn (1992) pointed out that the relative intensity of the fluctuations decayed towards zero downstream in this case. In Fig. 1, the relative intensity for GLS reaches an apparently near-constant value further downstream. Mylne and Mason (1991) also noted a near-constant relative intensity for both a 2m height source and a surface release in their field observations. Since the experiment range was up to 1000m, the 2m height source was unlikely to give results distinguishable from a surface release (Mylne and Mason, 1991). Hence both of the cases can be considered as a 'ground level source'. From the above LES data, wind tunnel measurements and field observations for GLS,

we speculate that the relative intensity further downstream becomes constant. This can also be deduced by using dimensional analysis. The concentration fluctuation intensity at ground level is related to the mean concentration C_m, the turbulence mixing scale L_t, the plume width L_c, the diffusivity K_m, the root of local total velocity variance $\varpi = \sqrt{\overline{u'^2} + \overline{v'^2} + \overline{w'^2}}$ and the Taylor scale L_λ at ground level, which can be expressed as $c_{rms} = f_0(C_m, L_t, L_c, K_m, \varpi, L_\lambda)$. The above equation can be simplified by using dimensional analysis,

$$\frac{c_{rms}}{C_m} = f(\frac{L_t}{L_\lambda}, \frac{\varpi L_c}{K_m}), \tag{3}$$

where $L_t = O(kz)$, k is von Karman's constant, z is the observation height, $L_c = O(x^{1/2})$. Note in equation 3 that the first factor L_t/L_λ is a constant at constant observation height. The second factor in Equation 3 can be rewritten as $O(x^{1/2}U)/\nu \times \varpi/U \times \nu/K_m$ and the full equation can be rewritten as follows,

$$\frac{c_{rms}}{C_m} = f_1(\frac{\varpi}{U} \times \frac{Ux^{1/2}}{\nu} \times Sc), \tag{4}$$

where the relative concentration fluctuation is related only to a single combined factor $x^{1/2}U/\nu$ multiplied by the relative r.m.s velocity and the Schmidt number Sc of the scalar. Recently Borgas et al. (2004) investigated a scalar fluctuation field generated by isotropic turbulence acting on a uniform mean gradient of scalar. They found that the non-dimensional scalar variance was a linear function of '$\ln Sc$'. For the GLS, the behaviour of scalar dispersion at source height in the far field might be similar to the above case. We rewrite Equation 4 as follows,

$$\frac{c_{rms}}{C_m} \approx \sqrt{c_0 + c_1 \times \ln(\frac{\varpi}{U} \times \frac{Ux^{1/2}}{\nu} \times Sc)}, \tag{5}$$

where c_0 and c_1 are constants. Note that as ϖ/U and Sc are constants at constant height, we get,

$$\frac{c_{rms}}{C_m} \propto \sqrt{\ln x^{1/2}}, \text{ for } x \to \infty. \tag{6}$$

The derivative of c_{rms}/C_m in Equation 6 is

$$\frac{d(c_{rms}C_m^{-1})}{dx} \propto \left[\ln(x^{1/2})\right]^{-1/2} \times x^{-1} \to 0, \text{ for } x \to \infty. \tag{7}$$

The concentration fluctuation relative intensity asymptotically tends to a constant in the far field.
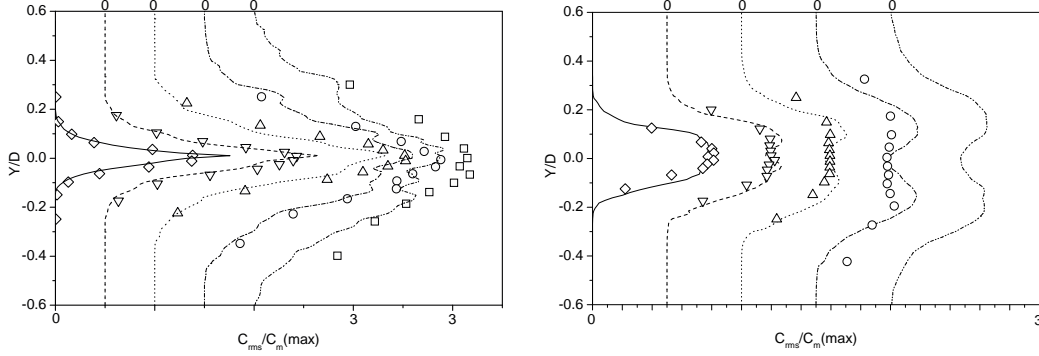
Fig. 2. Lateral profiles of $c_{rms}/C_m(max)$) at height of maximum concentration. Left ES; right GLS. Symbols, experiments, lines LES. — ⋄ x=0.575D, - - ▽ x=0.95D, ···· △ x=1.575D, -··- ∘ x=2.7D, -···- □ x=3.75D.

As is known (Borgas et al., 2004), in the far field the relative concentration fluctuation increases with increasing Schmidt number. In Equation 4, we deduce that f_1 is a increasing function of $\varpi/U \times Ux^{1/2}/\nu \times Sc$. Hence, c_{rms}/C_m decreases with decrease of ϖ/U. We assume that L_t/L_λ in Equation 3 is approximately a constant with height within some depth of the boundary layer, e.g. $D/2$. Hence, f_1 (Eq. 4) has approximately the same form at different heights. As the turbulence intensities decrease with increasing distance to the wall (Xie et al., 2004a), we might expect the asymptotic limit of the relative concentration fluctuation to decline with increasing source height, which is consistent with the above deduction for the GLS and Sykes and Henn (1992) results for the ES. However, the plume is likely to be mixed throughout the entire boundary layer in the far field and the effect of source height thus lost. Nevertheless, it is very likely that the asymptotic constant for the GLS is *not* zero.

The lateral profiles of c_{rms} are illustrated in Fig. 2. Note that the concentration r.m.s. is normalized by the maximum mean concentration at the same streamwise station. The comparison between the LES results and measurements is reasonable, though there are some random components in both at the far downstream positions, owing to the limited sampling time duration. Two peaks are seen in both the experimental and LES data for the lateral profile of c_{rms} for the GLS. We found that the maximum normalized c_{rms} at ground level occurred approximately at $y/\sigma_y=0.75$ for all downstream stations far from the source (beyond approximately $x/D=1.575$), where the lateral plume half-width σ_y was obtained by Gaussian fit. Since the turbulence scales in the near-wall region were much smaller than those far from the wall, meandering was much less for the GLS than the ES and any double peak structure in the ES was probably smoothed-out. Nevertheless, the double peak behaviour was more evident in the LES than that in experiment, which might possibly be related to a jet effect in the experiment or to a slight difference of the vertical location in the LES and in the experiment. Fackrell and Robins (1982) plotted

the lateral profiles of concentration variance at heights of 0.5 and 1.5 vertical-plume half-widths and the former show a maximum off the centreline while the latter do not. The current numerical results show a very similar behaviour.

The normalized scalar fluctuations spectra for the ES at three downstream stations, at the source height on the centreline, are plotted in Fig. 3(left). The measurements show a region with slope of approximately -0.7 preceding any -5/3 region that might exist, very similar to the wind tunnel data of Fackrell and Robins (1982). The roll-off of the spectra in the LES is clearly earlier than that in the spectra from the measurements. Similar evidence has also been found in the velocity spectra and discussed in our previous paper (Xie et al., 2004a), and is a direct consequence of the limited resolution in the LES. The roll-off in the LES spectra occurs in the frequency range where the slope in the experimental spectra is -0.7; of course, the LES data do not show this slope. The symbol $\vdash\!\dashv$ marks the dimensionless frequency of the inertial subrange on velocity spectra (Xie et al., 2004a). Note the Kolmogoroff scale at the source height was approximately 0.45mm (correspondingly $fD/U \simeq 480$), which was beyond the resolutions of both the experiment and the LES. The Batchelor scale is in the similar range assuming that the Schmidt number Sc is around 1.0 in the experiment and the LES.

A region with slope $-5/3$ is hard to discern in Fig. 3(left), which indicates that an inertial subrange behaviour does not exist. Warhaft (2000) summarized the scalar spectrum slope at various Reynolds numbers,R_λ, for shear flows and grid turbulence. For shear flows, there is a slow evolution toward $-5/3$, which is likely to be approached at large $R_\lambda(> 2000)$. For grid turbulence, the slope is close to $-5/3$ even at very low R_λ, e.g. 500. The Reynolds number in the experiments of Fackrell and Robins (1982) was approximately 3 times larger than that in the experiment reported here, which explains why the former measurements show a narrow (approximately one decade) $-5/3$ slope and ours do not. Mylne and Mason (1991) found a $-5/3$ slope over a range of frequencies between 0.01 Hz and 1 Hz (two decades) in a series of tracer experiments studying concentration fluctuations in a dispersing plume of pollutant in the atmosphere at ranges of between 200m and 1000m. Note that the Reynolds number of the field experiments was extremely high.

For dispersion from a point source in turbulent flows, the characteristics of the scalar fluctuation spectrum also depend on the distance from the source (Mylne and Mason, 1991). In the vicinity of the source, where the turbulence characteristic length scale L_η is large compared to the plume width L_c, the main role of turbulence acting on the plume is meandering. Turbulent eddies move the whole plume around producing periods of zero concentration in the time series measured at a fixed station. As the plume travels further downstream and L_c is of order L_η, the turbulent eddies of scale L_η dominate the growth of the plume and the generation of concentration variance. These

processes are in the stages described as 'molecular diffusion' and 'turbulent convection' by Brethouwer et al. (1999). Only in the third stage 'turbulent diffusion', where L_c is much larger than L_η, does turbulence mixing become dominant within the plume and the concentration variance is effectively transferred from low frequencies to high frequencies, developing an inertial subrange in the scalar spectrum. Mylne and Mason (1991) did not find a clear $-5/3$ slope in the spectrum of a time series taken at a short distance from the source (< 100m). However, as mentioned above, they did find a $-5/3$ slope over a wide range of frequencies at ranges between 200m and 1000m.

The normalized scalar spectra for the GLS at three downstream stations, which were located near the edge of the surface layer on the centre cross section, are plotted in Fig. 3(right). Again, the symbol $\vdash\dashv$ marks the dimensionless frequency of the inertial subrange on velocity spectra. Note the Kolmogoroff scale in the surface layer was approximately 0.17mm (correspondingly $fD/U \simeq 2700$), which was far beyond the resolutions of both the experiment and the LES. Both the LES results and measurements show a region with slope approximately -1 preceding any -5/3 region that might exist. As for the ES, the characteristics of the scalar spectrum depend on position in the plume. Fackrell and Robins (1982) also observed a significant region with slope approximately -1 (they suggested a value of -1.2) prior to a narrow $-5/3$ region for a GLS. Neither the present measurements nor the LES results show clearly a region with $-5/3$ slope. Fackrell and Robins (1982) measurements do show a narrow $-5/3$ region for the GLS because the Reynolds number of their experiment was approximately 3 times larger than that of the present experiment. Again, in the Mylne and Mason (1991) field measurements, both of the cases (2 m height source and ground level source) can be considered as a 'ground level source' in the far field. Their measurements show a wide region with $-5/3$ slope, which reflected the extremely large Reynolds number of the field work.

5 Methodology of EVT

The Generalized Pareto Distribution (GPD) (Davison and Smith, 1990) was used to predict extreme events exceeding a high threshold u in the time series:

$$Prob(\Gamma \le u + \phi \mid \Gamma > u) = G_{\xi\sigma}(\phi) = 1 - (1 + \frac{\xi}{\sigma}\phi)^{-1/\xi} \tag{8}$$

where Γ is the physical quantity, ϕ, ξ and σ are argument, shape and scale parameters respectively, and $\sigma > 0$, $\phi > 0$, $1 + \xi\phi/\sigma > 0$. ξ, σ are fitted by using the likelihood method (Davison and Smith, 1990). It is known that ξ is independent of u, while σ depends linearly on u and that $\xi < 0$ for the GPD to have a finite upper limit (Munro et al., 2001).
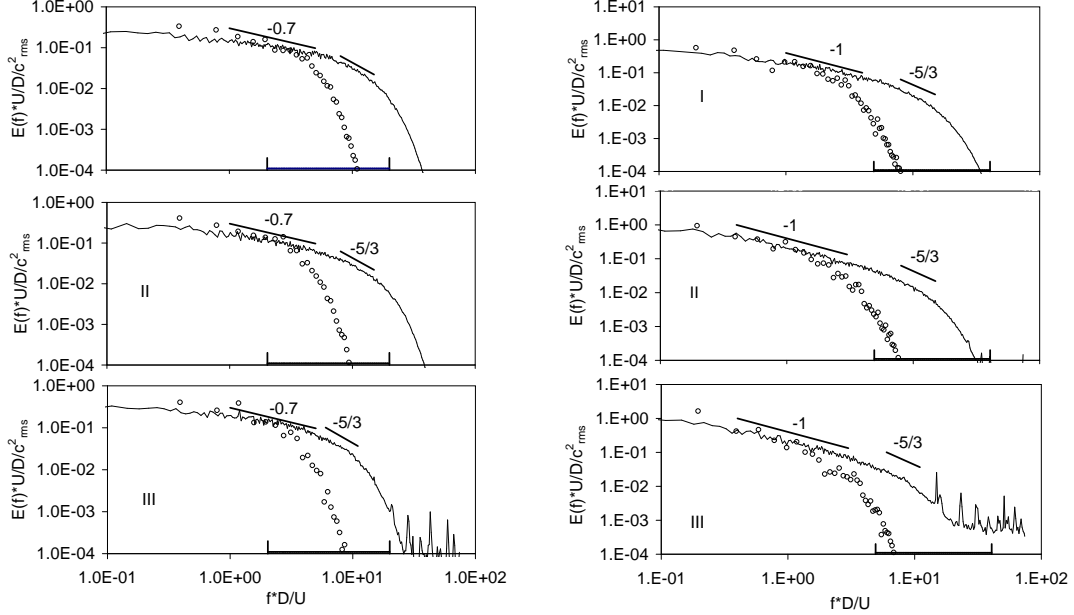
Fig. 3. Spectra of concentration fluctuations. I at x=0.575D, II at x=1.575D, III at x=2.7D; all at y=0. ∘ LES; —— measurements. ⊢⊣, mark of inertial subrange on velocity spectra (Xie et al., 2004a). Left: ES, at source height. Right: GLS; LES at z=0.096D; measurements at z=0.05D, 0.0625D and 0.134D respectively in I, II and III.

The mean excess function of the GPD distribution was used as the diagnostic tool to choose a proper threshold u,

$$E(\Gamma - u|\Gamma > u) = \frac{\sigma + \xi u}{1 - \xi}, \tag{9}$$

provided $\xi < 1$. In practice, the threshold is chosen from a mean excess plot in which the mean difference between the exceedances and the threshold is plotted against the threshold. Within some range of the threshold u, ξ is independent of u, where the asymptotic approximation is valid. The mean excess plot should be a straight line with slope $\xi/(1-\xi)$ and intercept $\sigma/(1-\xi)$. Nevertheless, it only provides a necessary but not sufficient condition for fixing the threshold. Quantile quantile (QQ) plots can also be used to find a suitable threshold, and to check the goodness of fit.

For a threshold u, let τ denote the time period, ν is the crossing rate of the threshold u and r is the return level (note $r > u$). From equation 8, the average crossing rate of level r is $\nu \left[1 + \xi(r - u)/\sigma)^{-1/\xi}\right]$, which is set equivalent to $1/\tau$ to readily obtain

$$r = u - [1 - (\nu\tau)^{\xi}]\sigma/\xi. \tag{10}$$

Theoretically, the return level r is independent of the threshold u. Provided $\xi < 0$, the local maximum (upper limit) is deduced from the above equation as,

$$\Gamma_0 = u - \sigma/\xi. \tag{11}$$

The data for processing by EVT are assumed to be independent and identically distributed (IID). However, since the turbulent fluctuation is not fully random, data obtained from LES and experiment are not truly independent and identically distributed (IID). Although the assumption of dependence is not crucial, it's contravention will affect the ability to calculate reliable confidence intervals (Munro et al., 2001). A technique of "decluster" is applied to pre-process the data before a GPD is fitted (Davison and Smith, 1990; Mole et al., 1995; Munro et al., 2001; Smith, 1989; Xie et al., 2004b), where the key is to specify a threshold u and a cluster time interval T_c.

6   Data to be processed by EVT

For LES data there were 7 output stations for GLS and 5 output stations for ES respectively, while for the experiments there were 5 output stations for GLS and 5 output stations for ES respectively (see Tables 1 and 2). Table 1 is a summary of the time series for ES, where enes are numerical data, and exes are experimental data. The output positions were located at the height of source. The sampling duration T_{tlt} and frequency were 5 minutes and 1000 Hz for the experiment. Table 2 is a summary of the time series for GLS, where the output positions of gngs (LES) and gxgs (experiment) were located close to ground-level. In addition, there were 5 output stations at $x/D = 7.8$ (at $z/D =$0.00784, 0.09593, 0.18024, 0.31361, 0.44022) in the LES. Note that all of the output locations were in the same vertical section ($y = 0$). Since the dimensionless size of the LES time series was shorter than that from the experiments, all of the time series from LES have been carefully assessed by checking the sampling errors. The maximum differences of concentration fluctuation $r.m.s$ between the short duration "sub-series" (13.6%, 27.3%, 54.5% and 81.8% of the total) and the total were found to be less than 10%. Assessed by the same procedure, the sampling errors of the time series from the experiment were quite satisfactory.

Table 1
Summary of LES and experimental time series for ES

LES,$H_s/D = 0.432, T_{tlt} \times U/D = 550$					Exp,$H_s/D = 0.444, T_{tlt} \times U/D = 1950$				
series	ene1	ene2	ene3	ene4	ene5	exe1	exe2	exe3	exe4	exe5
x/D	0.575	0.95	1.575	2.7	3.75	0.575	0.95	1.575	2.7	3.75

*H_s source height,T_{tlt} sampling duration.

Table 2
Summary of LES and experimental time series for GLS

LES,$H_s/D = 0.00784, T_{tlt} \times U/D = 550$			Exp,$H_s/D = 0.00698, T_{tlt} \times U/D = 1950$		
series	x/D	z/D	series	x/D	z/D
gng1	0.575	0.00784	gxg1	0.575	0.02635
gng2	0.95	0.00784	gxg2	0.95	0.02635
gng3	1.575	0.00784	gxg3	1.575	0.02635
gng4	2.7	0.00784	gxg4	2.7	0.02635
gng5	3.75	0.00784	gxg5	3.75	0.02635
gng6	6.0	0.00784			
gng7	7.8	0.00784			

7 Some EVT results

In order to validate the fitting process, for each series we chose several different cluster time intervals T_c and thresholds u, and checked the fitted parameters, the standard errors and the estimated local maxima. Some typical examples of the comparisons are shown in Table 3. We found that the sensitivity to T_c and u to the EVT parameters was weak. In particular, the local maxima Γ_0 were fairly stable. Note the maximum concentration was not dimensionless. The mean excess plots and quantile-quantile (QQ) plots were also checked. The optimum (T_c, u) were chosen as (0.25, 3.36), (0.25, 0.11), (0.325, 500) for gng1, gng7 and gxg1 respectively. The shape parameter ξ tended to decrease with downstream distance, which can be interpreted in terms of meandering and intermittency becoming weaker further downstream.

Several typical mean excess plots and QQ plots for gxgs are shown in Fig. 4. The plots are acceptable, suggesting that the fitting process is a success. We noted that there was a broad area with nearly constant slope on the mean excess plots. In order to check the robustness of prediction, the GPD parameters generated from fits to various durations of data, up to the maximum gathered, were compared. These series with different durations were processed using the same threshold and cluster time interval. The parameters of ξ and σ and the

Table 3
Examples of comparisons among different cluster time intervals T_c and thresholds u.

	$T_c \times U/D$	$u \times 1000$	ξ(s.e)	σ(s.e.)$\times 1000$	$\Gamma_0 \times 1000$
	0.125	2.5	-0.1112(0.0871)	7.292(0.136)	68.05
	0.125	3.36	-0.09647(0.0101)	6.865(0.137)	74.53
	0.125	4.0	-0.08434(0.0113)	6.564(0.138)	81.82
gng1	0.25	3.36	-0.1123(0.0129)	7.613(0.205)	71.19
	0.25	0.08	-0.3403(0.0173)	0.07521(0.00220)	0.3010
	0.25	0.11	-0.2646(0.0257)	0.05687(0.00221)	0.3250
	0.25	0.14	-0.2444(0.0378)	0.04741(0.00257)	0.3340
gng7	0.5	0.11	-0.2810(0.0356)	0.05989(0.00321)	0.3231
	$T_c \times U/D$	u	ξ (s.e)	σ (s.e.)	Γ_0
	0.325	450	-0.1346(0.0103)	271.3(5.2)	2465
	0.325	500	-0.1104(0.0125)	249.2(5.3)	2755
	0.325	550	-0.0850(0.0151)	230.5(5.6)	3230
gxg1	0.65	500	-0.1517(0.0153)	294.2(8.6)	2438

local maximum Γ_0 were studied as functions of the duration of data used for the fitting process. We found that the parameters tended to constants for the longer series durations, demonstrating the process was robust.

The relative maximum is defined as the maximum concentration (upper limit Γ_0) normalized by the local maximum mean concentration C_m. Fig. 5(top) illustrates the comparison of the relative maxima between enes and exes. Despite the large confidence interval of enes, the relative maxima for enes are in good agreement with that for exes in Fig. 5. Compared with those for the GLS, both the magnitude and the trend against downstream distance for the ES in Fig. 5 are absolutely different (the upper limit Γ_0 can be even more than 50 times larger than the mean concentration for the ES), which suggests that the turbulence has a large effect on the extreme concentrations, since the local turbulence in the near wall region is quite different from that at the height of the ES. It is expected that the relative maxima will remain at a large level for a long distance downstream from $x/D = 3.75$, which is quite different from the case of the GLS.

Fig. 5 (bottom) also shows the comparison between LES and experiment of the relative maxima at several downstream locations for the GLS. The comparison is quite reasonable. We found that the local maximum Γ_0 far downstream was approached by the 'return level' in a shorter 'return period' than close to

13
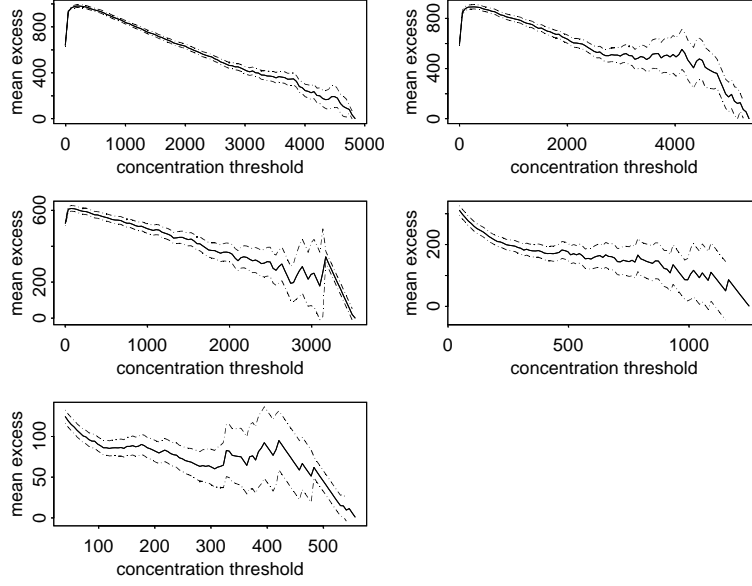
(a) Mean excess plots.
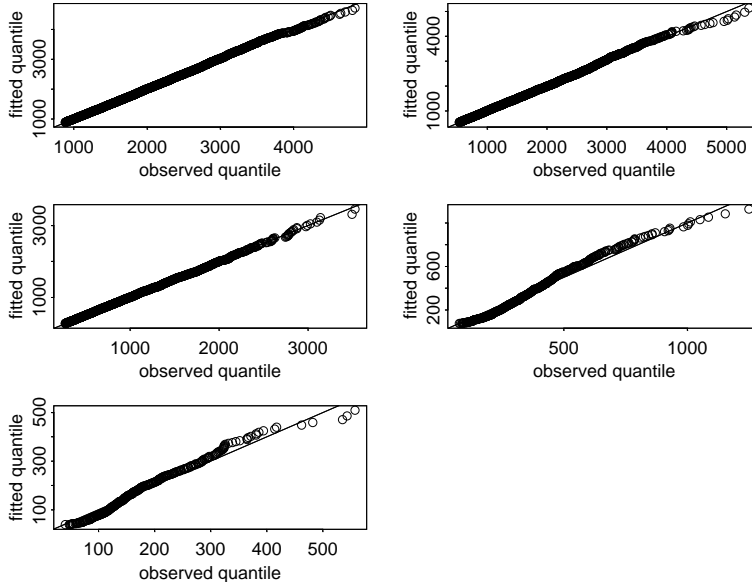
(b) Quantile-quantile plots.

Fig. 4. From left to right then top to bottom: exe1, exe2, exe3, exe4, exe5. (a) Solid lines, mean excess; dash dot lines, 95% confidence interval.

the source (see Eq. 10 and 11). Note the time series far downstream were "denser"(fewer zero or very low concentration value and more peaks) due to the weak meandering, which generated a lower ξ (see gng1 and gng7 in Table 3) and made the return period less at the same return level. In Fig. 1 the relative intensity of the LES data and measurements for the GLS shows a very slight decay around $x/D = 1.0$ whereas further downstream, from $x/D = 2.0$, it

14
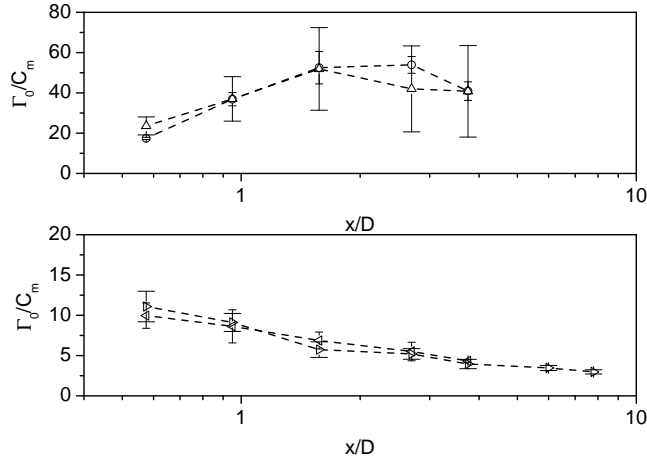
Fig. 5. Relative maximum concentrations. Top: $--\triangle--$ ES LES;$--\circ--$ ES measurements. Bottom: $--\triangleright--$ GLS LES;$--\triangleleft--$ GLS measurements. Vertical bars: 95% confidence intervals, large cap, LES; small cap, measurements.

clearly approaches a very evident constant. However in Fig. 5 (bottom), the relative maximum shows a slow decay with downstream distance, which does not have an obvious limit. We see that Fig. 5 for the ES is very similar in shape to the plot of relative intensity of fluctuations for the ES (see Fig. 1), where the peak is also located around $X/D = 2.0$. Again, Sykes and Henn (1992) argued that the relative intensity of turbulence fluctuations for the ES decays towards zero downstream. In Fig. 5 (top) for the ES, there is an evident decay downstream.

In order to investigate further the similarity between the relative maxima Γ_0/C_m and the relative intensity of fluctuations c_{rms}/C_m, a plot of Γ_0/c_{rms} against the downstream distance is illustrated in Fig. 6. Note for the ES that further downstream from $x/D = 0.95$, the numerical and experimental curves converge approximately to a constant value of 20, which confirms that the relative maxima and the relative intensity of fluctuations against the downstream distance are similar in shape in the far field. For the GLS, it is only further downstream from approximately $x/D = 3.75$, that the decline with the downstream distance slows down significantly. Note that the sudden decay at the furthest point in the experimental data is due to background instrument noise significantly affecting c_{rms} (Xie et al., 2004b). Nevertheless, it seems that there is a similarity in shape between the relative maxima and the relative intensity against the downstream distance for the GLS, in particular in the far field, where the numerical data converge approximately to a constant value of about 6.

The vertical profiles of the local maxima at $x/D = 7.8$ obtained from LES for the GLS are plotted in Fig.7, where $C_{lm}(z)$ is the local mean concentration at height z, C_m is the maximum mean concentration at the streamwise location

15
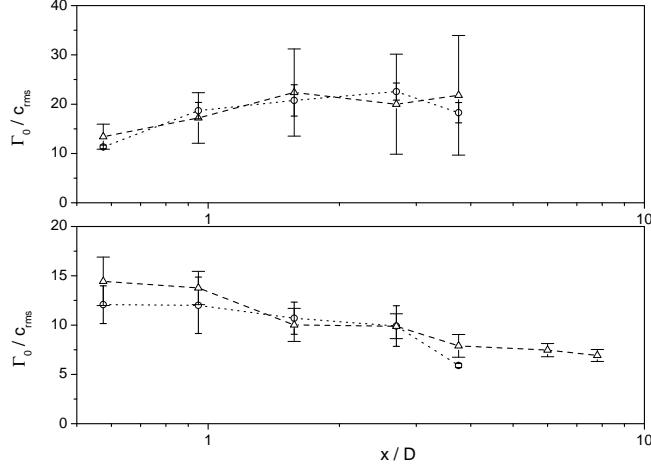
Fig. 6. Upper limit Γ_0 normalized by c_{rms}: Left, ES; right, GLS. $--\triangle--$ LES; $\cdots\circ\cdots$ measurements. Vertical bars: 95% confidence intervals, large cap, LES; small cap, measurements.
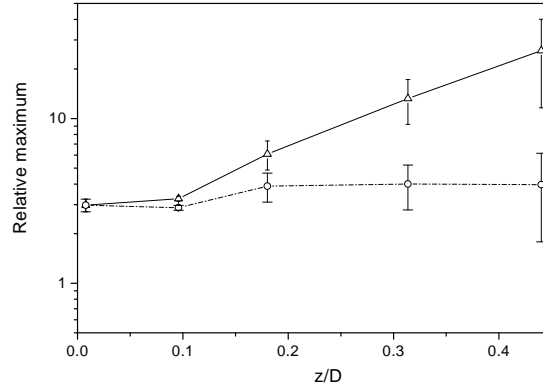
Fig. 7. Vertical profiles of local maxima at x/D=7.8. GLS, LES. Vertical bars: 95% confidence intervals; $-\!\triangle\!-$ $\Gamma_0(z)/C_{lm}(z)$; $-\!\cdot\!-\circ\!-\!\cdot\!-$ $\Gamma_0(z)/C_m$.

$x/D = 7.8$. The normalized half width of the plume σ_z/D is 0.26. Note that the predicted highest concentration is not found at the core of the plume, but, instead, at the edge. Further, we found that the local largest concentration in the long-term numerically simulated time series at the top of the surface layer was greater than that at ground level (in the core of the plume). This is mainly because at the top of surface layer, although the distance to the source was slightly longer than that at the core at the same streamwise location, the background mean streamwise velocity was much larger and hence the dispersion time was less than that at the core. Also the turbulence intensities were larger at ground level than well away from the wall. Larger turbulence intensities enhance the turbulent mixing, which diminishes the local maximum concentration.

16

8 Conclusions and discussions

The relative concentration fluctuations, demonstrated by vertical and lateral profiles of fluctuation r.m.s for a GLS and ES obtained from LES were in good agreement with measurements. We stress again that modelling fluctuations for the GLS in particular is a hard task (Sykes and Henn, 1992). For the ground-level source, the relative intensity of the concentration fluctuations reached an apparently near-constant value further downstream. It has been speculated (Sykes and Henn, 1992) that this was found in field observations because of the presence of the large scale eddies in the atmosphere. For the wind tunnel experiment and our numerical simulation, the ratio of the dominant eddies near the wall (e.g. GLS) to the largest eddy was much smaller than that far from the wall. Hence the numerical simulation and wind tunnel experiments for the GLS were in similar situation to Mylne and Mason (1991) field observations. Furthermore, dimensional analysis was used to estimate the downstream trend for the GLS. This confirmed that the relative intensity approached a constant value downstream.

Frequency regions with slope approximately -1 in the spectra for the GLS and of -0.7 for the ES were observed in the current study. These preceded any -5/3 region that might exist, though, in fact, none of the spectra showed a clear $-5/3$ region. On the basis of this study, we were confident that the current LES model was reliable for calculating dispersion from sources in turbulent boundary layer flow, and can be applied to further analysis, such as the prediction of extreme events and their return periods.

Twenty six time series, which were collected at ground-level for the GLS and at the source height for the ES, were processed successfully by using the Generalized Pareto Distribution to predict the occurrence of rare events. A remarkable difference in the character of the extreme concentrations was found between the elevated source release and the ground-level source release, suggesting that the turbulence characteristics played a very important role in the extreme concentration. From the vertical profiles of the local maxima for the GLS, the predicted highest concentration was not found at the core, but at the upper edge of the plume.

It was noted that the variations of the relative concentration maxima with the downstream distance were more or less similar in shape to the equivalent relative intensity variations. Both the relative maxima and the relative intensity plots for the ES indicated decay towards zero in the very far field, though whether this trend will persist is unclear. For the GLS, the relative intensities approached a clear far field limit whereas the behaviour of the relative maxima was less obvious, with perhaps some sign of slow far field decay. A question arising here is: is there any similarities or simple relations between the relative

maxima and the relative intensities (or higher order moments)? If so, a lot of effort could be saved in obtaining the relative maxima.

Acknowledgment

References

Anderson C.W., Mole N. and Nadarajah S., 1997. A switching Poisson process model for high concentration in short-range atmospheric dispersion. *Atmospheric Environment* **31**, 813-824.

Borgas M.S., Sawford B.L., Xu S., Donzis D.A. and Yeung P.K., 2004. High Schmidt number scalars in turbulence: structure functions and Lagrangian theory. *Phys. Fluids* **16** (11), 3888-3899.

Brethouwer G., Boersma B.J., Pourquié M.B.J.M and Nieuwstadt F.T.M.,1999. Direct numerical simulation of turbulent mixing of a passive scalar in pipe flow. *Eur. J. Mech. B Fluids* **18**, 739-756.

Coles S.G.,2001. An introduction to statistical modelling of extreme values. *Springer*.

Davison A.C. and Smith R.L., 1990. Models for exceedances over high thresholds (with discussion). *J. R. Statist. Soc. B* **52**, 393-442.

Fackrell J.E. and Robins A.G.,1982. Concentration fluctuations and fluxes in plumes from point sources in a turbulent boundary layer. *J. Fluid Mech.* **117**, 1-26.

Mole N., Anderson C.W., Nadarajah S. and Wright C.,1995. A generalised Pareto distribution model for high concentration in short-range atmospheric dispersion. *Environmetrics* **6**, 595-606.

Munro R.J., Chatwin P.C. and Mole N., 2001. The high concentration tails of the probability density function of a dispersing scalar in the atmosphere. *Boundary-Layer Meteorol* **98**, 315-339.

Mylne K.R. and Mason P.J.,1991. Concentration fluctuation measurements in a dispersing plume at a range of up to 1000 m. *Q.J.R. Meteorol. Soc.* **117**, 177-206.

Pickands J.,1975. Statistical inference using extreme order statistics. *Ann. Statist.* **3**, 119-131.

Smith R.L., 1989. Extreme value analysis of environmental time series: an application to trend detection in ground-level ozone. *Statistical Science* **4** 367-393.

Sykes R.L. and Henn D.S.,1992. LES of concentration fluctuations in a dispersing plume. *Atmospheric Environment* **26A**, 3127-3144.

Thomson D.J.,1990. A stochastic model for the motion of partical pairs in isotropic high-Reynolds-number turbulence, and it application to the problem of concentration variance, *J. Fluid Mech.*, **210**, 113-153.

Warhaft Z., 2000. Passive scalars in turbulent flows. *Ann. Rev. Fluid Mech.* **32** 203-240.

Waterson N. P. and Deconinck H., 1995 A unified approach to the design and application of bounded higher-order convection schemes, in 'Numerical Methods in Laminar and Turbulent Flows'. *Proceedings of the Ninth International Conference* (ed. Taylor C. and Durbetaki P.) **9** Part 1 203-214.

Xie Z., Voke P.R., Hayden P. and Robins A.G.,2004a. Large-eddy simulation of turbulent flow over a rough surface. *Boundary-Layer Meteorol.* **111** 417-440.

Xie Z., Hayden P., Voke P.R. and Robins A.G., 2004b. Large-eddy simulation of dispersion: comparison between elevated source and ground level source. *J. Turbulence.* **5**(31) 1-16.